**Light Metals 2013** *Edited by: Barry Sadler*
***TMS (The Minerals, Metals & Materials Society), 2013***

# MAGNETOHYDRODYNAMIC MODEL COUPLING MULTIPHASE FLOW IN ALUMINUM REDUCTION CELL WITH INNOVATIVE CATHODE PROTRUSION

WANG Qiang, LI Baokuan, WANG Fang, FENG Naixiang
School of Materials and Metallurgy, Northeastern University, Shenyang, Liaoning, 110819, P.R.China

Keywords: Innovative Cathode Protrusion, Magnetohydrodynamic calculation, Multiphase, Aluminum Reduction Cell

## Abstract

The electromagnetic field and the gas bubbles generated beneath anodes in aluminum reduction cells have an important role in the fluctuation of the bath/metal interface. A coupled mathematical model has been developed to investigate the electromagnetic field and the multiphase flow in the aluminum reduction cell with innovative cathode protrusion. As for the electromagnetic field, the finite element method was employed. A transient inhomogeneous multiphase model, the finite volume method, was employed to study the multiphase flow. The results indicated that the electromagnetic field distribution was changed by the innovative cathode protrusion. The electromagnetic force decreased as a result of the optimization of the magnetic field. In addition, the deformation of the metal/bath interface was suppressed significantly, which is beneficial to the reduction of the voltage drop. The innovative cathode protrusion had little effect on the motion of the gas bubbles.

## Introduction

The Hall-Héroult process is the main industrial process for the production of primary aluminum. Alumina powder is dissolved in the bath. A direct current is applied and passes through the entire reduction cell. In this process, the interaction of magnetic field with the current produces an EMF which causes fluctuation of the molten fluid. In addition, because of the electrochemical reaction, carbon monoxide and carbon dioxide form at the bottom of the anode, and induce molten fluid motion in the process of floating up to escape. Thus, the molten fluid motion is due to the combined effect of the EMF and the gas bubbles generated at the anode.

The process of aluminum electrolysis costs lots of electric energy. Stable and efficient operation of the electrolysis process involves the removal of anode gas bubbles and the oscillation of the metal-bath interface. Many researchers have been made to study the interface deformation. Severo et al. [1] developed a 3-D model by coupling commercial software ANSYS and CFX. By using the homogeneous model, they calculated the flow field and interface deformation of metal. But they ignored the anode gas bubbles that also contributes to the interface deformation. Li et al. [2] studied the flow characteristics and the vortex structures of the molten fluid in the aluminum reduction cell by using the method of vorticity and swirling strength. The results reveal that, compared with velocity vector distribution and streamline picture, this method can provide more flow field information. Vortexes usually occur as reverse symmetrical pairs. The single factor comparative study shows that the EMF tends to trigger large vortexes near the upstream side, while gas bubbles mainly stir the bath and generate small vortexes.

Recently a low energy consumption aluminum reduction cell with novel protrusion, as show in Fig.1, was proposed by Feng [3]. The results of industrial experiments showed that the electric power is reduced by more than 1200 kWh for every ton of aluminum with the help of this novel cathode. In this paper, the electromagnetic field and melt flow-related phenomena in the new reduction cell with novel protrusion was studied using a coupled mathematical model. This paper provides the theoretical basis for the optimization of the novel cathode.

Fig. 1 Structure of the novel cathode

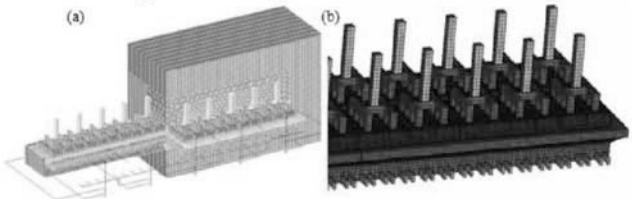


Fig. 2 Computational mesh of the 300 kA cell with novel cathode

## Mathematical Model

In order to simplify the problem, some assumptions are made as follows:

(1) Currents applied to each anode are equal;
(2) Results are predicted for steady state condition;
(3) The effect of molten fluid flow on the magnetic field is negligible;
(4) Gas bubble is regarded as continuous phase.

Electromagnetic model

The governing equations that are used are Maxwell equations as follow:

Ampere law: $$\nabla \times \vec{H} = \vec{J} + \frac{\partial \vec{D}}{\partial t} \quad (1)$$

Faraday law: $$\nabla \times \vec{E} = -\frac{\partial \vec{B}}{\partial t} \quad (2)$$

Gauss law: $$\nabla \cdot \vec{D} = \rho \quad (3)$$

Constitutive equation of magnetic flux is

$$\nabla \cdot \vec{B} = 0 \quad (4)$$

The Lorentz force is then evaluated as a vector cross product of the current vector and the magnetic flux density vector in molten aluminum using following relation.

$$F_x = J_y \cdot B_z - J_z \cdot B_y$$
$$F_y = J_z \cdot B_x - J_x \cdot B_z \quad (5)$$

$$F_z = J_x \cdot B_y - J_y \cdot B_x$$

$$F_n = \sqrt{F_x^2 + F_y^2 + F_z^2}$$

where $\vec{H}$ is magnetic field intensity; $\vec{J}$ is total current density vector; $\vec{D}$ is electric flux density vector; $\vec{B}$ is magnetic flux density; $\vec{E}$ is electric field intensity vector; $\rho$ is electric charge density; t is time.

Multiphase flow model

The three-phase flow in aluminum reduction cells was simulated by calculating the continuity equation and Navier-Stokes equations, using the standard *k-ε*, two-equation turbulent model.

Continuity equation:
$$\frac{\partial \rho}{\partial t} + \frac{\partial (\rho u_i)}{\partial x_i} = 0 \quad (6)$$

Navier-Stokes equation:
$$\frac{\partial (\rho u_i)}{\partial t} + \rho \frac{\partial (u_i u_j)}{\partial x_j} = -\frac{\partial p}{\partial x_i} + \frac{\partial}{\partial x_j}\left(\mu_{eff} \frac{\partial u_i}{\partial x_j}\right) + \frac{\partial}{\partial x_j}\left(\mu_{eff} \frac{\partial u_j}{\partial x_i}\right) + \rho g + \vec{F} \quad (7)$$

where $\rho$ is density; t is time; $u_i$ is velocity component in $x_i$ direction; p is pressure; $\vec{F}$ is a momentum source used to incorporate the electromagnetic force; $\mu_{eff}$ is the turbulence-adjusted effective viscosity.

The volume of fluid (VOF) multiphase model was employed to track the free surface moving through the computational grid by simultaneously solving another parameter - the volume of fluid per unit volume $f_i$. It requires the addition of the following conservation equation:

$$\frac{\partial f_i}{\partial t} + \left[\frac{\partial}{\partial x_i}(f_i u_i)\right] = 0 \quad (8)$$

The VOF method was used to solve the fluid flow problems. It is an efficient algorithm for free surface tracking. This approach has a powerful volume-tracking feature.

**Boundary Conditions**

The commercial package ANSYS, which is based on the finite element method, is used to analyze the electromagnetic field and the current field system. The nodal-based method (Solid117 element type) is used to solve three–dimensional static electromagnetic field. The current amplitude loaded on the upper surface of the guide rod of anode is 300kA with coupled VOLT freedom, and the electric potential on the top surface of the steel bars is zero. The relative permeability of the conductor is set to 1. The inlet is applied a velocity inlet. The pressure outlet boundary condition is used for the outlet. No slip wall was used for the gas bubble and the bath on the anode surface. In contrast, free slip wall was used for the gas bubble on the other surfaces because the gas bubbles on them are very sparse. Moreover, no slip wall was used for the bath and the metal on the other surfaces. The physical properties, geometrical and operating conditions are shown in Table 1 and Table 2.

Table1 Geometry and operating parameters of the aluminum reduction cell

| Geometry /m | | Parameter | |
|---|---|---|---|
| Chamber | 14.85×4.20×1.34 | Current / kA | 300 |
| Anode carbon | 1.64×0.66×0.55 | Voltage / V | 4 |
| Cathode | 3.44×0.51×0.45 | Number of bar | 26 |
| Cathode Bus | 1.57×0.18×0.13 | Number of buss | 26 |

Table 2 Physical parameters for electromagnetic field calculation

| Parameters of electrical($\Omega \cdot m$) | |
|---|---|
| Resistance of molten aluminum | $2.4\times10^{-7}$ |
| Resistance of electrolyte | $4.5\times10^{-3}$ |
| Resistance of carbon anode | $3.5\times10^{-5}$ |
| Resistance of steel stubs | $2.34\times10^{-7}$ |
| Resistance of cathodes | $3.8\times10^{-5}$ |
| Resistance of the cathode bar | $7.78\times10^{-7}$ |

**Results and Discussion**

The total current density distribution of (a) a traditional aluminum reduction cell, and (b) the innovative aluminum reduction cell is shown in Fig.3. The current density distribution of the innovative aluminum cell is more uniform than that of the traditional aluminum cell, since the current would be redistributed with the help of the protrusion in the innovative cathode. Because the current density becomes more uniform in the innovative aluminum reduction cell, the cell voltage drop of the innovative aluminum reduction cell is decreases which is beneficial to the energy saving.

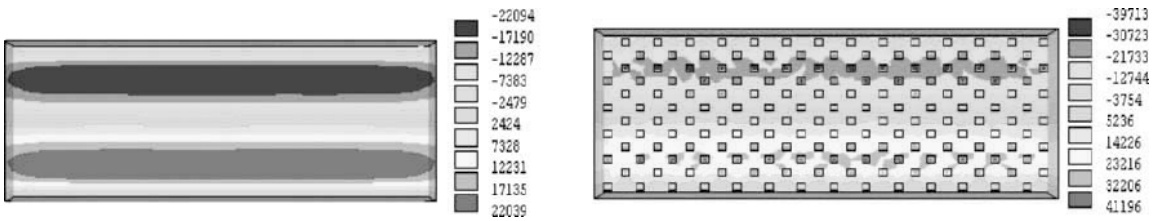


(a) traditional aluminum cell (b) innovative aluminum cell

Fig. 3 The total current distribution on the bottom surface of molten aluminum along X direction

The current density of different sections in the two cells are symmetrical, and current increases gradually outward from the center, in accordance with the regulation of the current distribution in electrolytic cell, as shown in Figure 4.

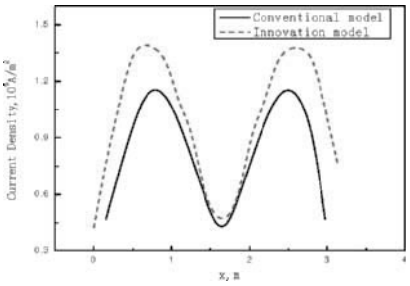


Fig. 4 The current density distribution on the center section of molten aluminum in the tradition and innovative aluminum cell

The magnetic flux density $B_x$, $B_y$ and $B_z$ distribution in molten aluminum in the traditional and innovative aluminum cells are shown in Fig.5-6. From these pictures, we can see that the magnetic flux density $B_x$ is inverse symmetrical along the short axis. The magnetic flux density $B_y$ is inverse symmetrical along the short axis, but is symmetrical along the long axis. The magnetic flux density $B_z$ is inverse symmetrical distribution along the short axis. The distribution of magnetic flux density in the two designs is similar. However, the magnetic flux density $B_x$, $B_y$ in the innovative aluminum reduction cell is less than that in the traditional aluminum reduction cell. The magnetic flux density $B_z$ in the innovative aluminum reduction cell is slightly greater than that in the traditional aluminum reduction cell. The pictures indicate that the EMF in the traditional aluminum reduction cell is greater than that in the innovative aluminum reduction cell.

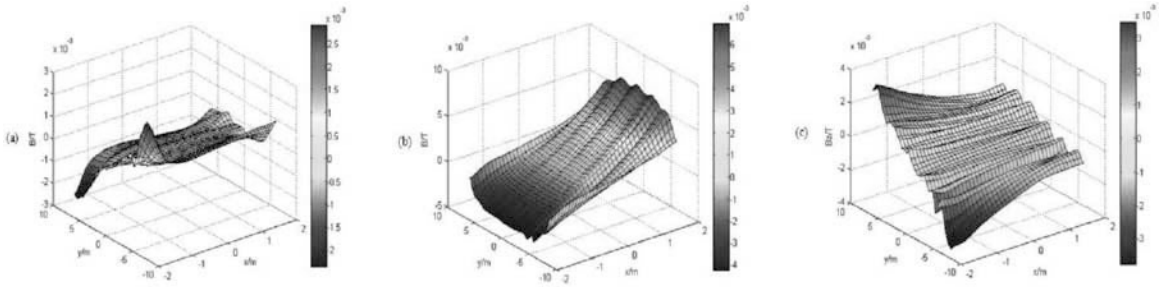

Fig. 5 The magnetic flux density distribution of molten aluminum in the traditional aluminum cell

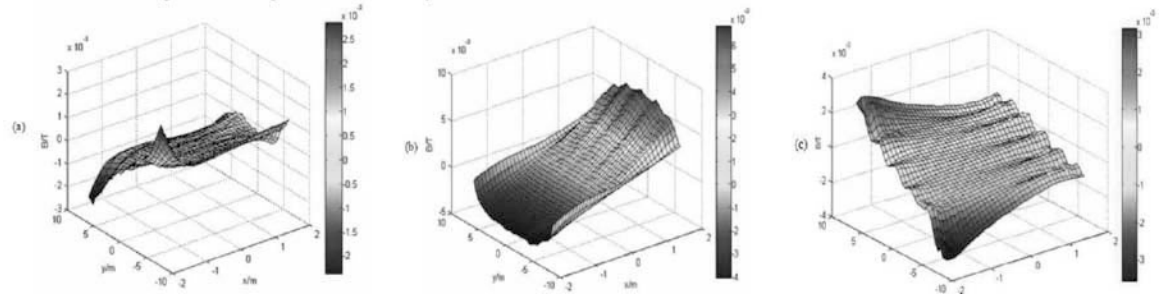

Fig. 6 The magnetic flux density distribution of molten aluminum the innovative aluminum cell

In order to investigate the mechanism of how the interface becomes flat under the effect of the novel cathode protrusion, the EMF is calculated as shown in Fig.7. The EMF is an important driving force for the deformation of the interface, and also decreases under the effect of the novel cathode protrusion. The magnetic induction reduces as a result of the optimization of the magnetic field due to the novel cathode protrusion. Moreover, the effect of the EMF would negate each other because of the direction of the EMF is inconsistent around the cathode protrusion.

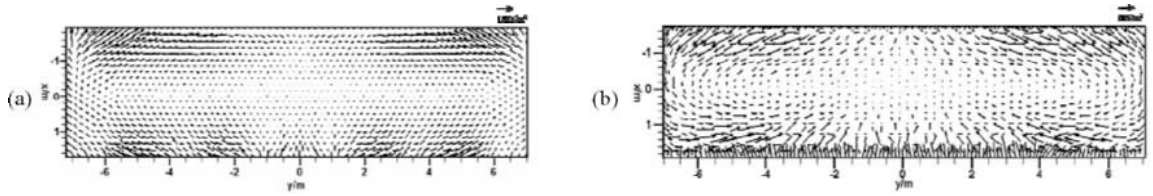


Fig.7 Distribution of the horizontal EMF in the metal melt layer: a) without novel cathode protrusion, b) with novel cathode protrusion

The deformation of the metal-bath interface is shown in Fig.8. The deformation degree of the interface in the reduction cell without the novel cathode protrusion is bigger than that in the reduction cell with the novel cathode protrusion. In the reduction cell without the novel cathode protrusion, the biggest hump of the interface is located at the two sides of the reduction cell under the effect of the two reverse symmetrical vortexes and the anode gas bubbles. However, the big hump disappears in the reduction cell with the novel cathode protrusion and the interface becomes flat. It can be inferred that the novel cathode protrusion can reduce the fluctuation significantly. Hence, the ACD can be decreased in the reduction cell which provides

benefits in electric energy saving.

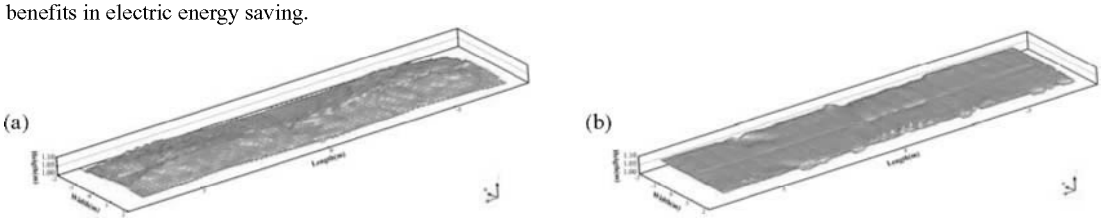


Fig.8 Deformation of the metal-bath interface: a) without novel cathode protrusion, b) with novel cathode protrusion

In another aspect, the flow field and the metal velocity swirling strength of the metal layer are shown in Fig.9. The swirling strength is a mathematical tool to measure the strength vortex, i.e. the higher the local swirling strength, the stronger the fluid vortex [6]. In the reduction cell without the novel cathode protrusion, the metal flow velocity is very high and two reverse symmetrical vortexes can be clearly observed which would generate a strong stirring. The maximum metal velocity swirling strength is 0.952 $s^{-1}$. Therefore, inevitably the interface would fluctuate sharply. On the contrary, the metal flow becomes very smooth in the reduction cell with the novel cathode protrusion and the metal flow velocity decreases by a wide margin. Although the two reverse symmetrical vortexes still exist, their strength and influence greatly reduce. It is mainly because the cathode protrusion plays a hindering effect on the flow of the metal. More importantly, the large vortex in the metal flow field would break up into the small vortexes by the cathode protrusion and then dissipated due to the viscous force and the hindering effect of the cathode protrusion. This theory can be validated through Fig.9 (b). The quantity of the vortex as well as the strength of the vortex reduces significantly. The maximum of the metal velocity swirling strength is 0.626 $s^{-1}$, lower than in the reduction cell without the novel cathode protrusion.

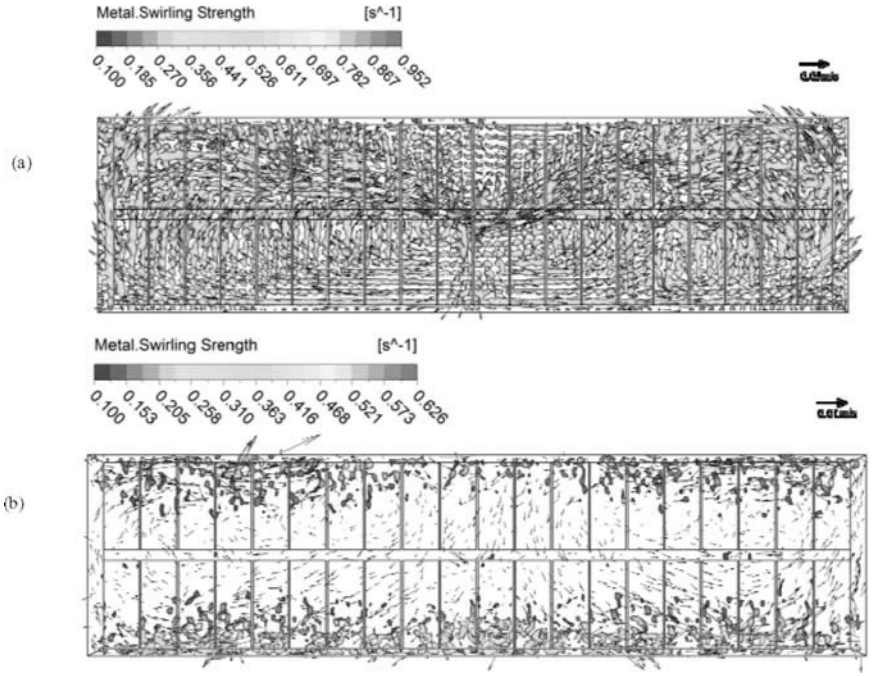


Fig.9 Flow field and the swirling strength of the metal melt layer: a) without novel cathode protrusion, b) with novel cathode protrusion

## Conclusions

(1) Because the current density becomes more uniform in the innovative aluminum reduction cell, the cell voltage drop of the innovative aluminum reduction cell is lower, which is beneficial to energy saving.

(2) The metal-bath interface deformation can be reduced significantly by the novel cathode protrusion, which is beneficial to electric energy saving.

(3) The EMF decreases as a result of the optimization of the magnetic field due to the novel cathode protrusion, which is an important driving force for the deformation of the interface.

(4) Large vortex in the metal flow field is broken up into small vortexes by the cathode protrusion and then dissipated due to the viscous force and the hindering effect of the cathode protrusion. The quantity of the vortex as well as the strength of the vortex reduces significantly in the reduction cell with the novel cathode protrusion.

## Acknowledgments

The project is supported by the National Natural Science Foundation of China (No.50934005) and the National Natural Science Foundation of China (NO. 50904014).

**References**


1. J. I. Buiza. Electromagnetic Optimization of the V-350 Cell . Light Metals 1989 , 211-214.

2. M. Dupuis and V. Bojarevics. Weakly Coupled Thermo-electric and MHD Mathematical Models of an Aluminum Electrolysis Cell. Light Metals 2005, 449-454.

3. V.Bojarevics and K.Pericleous. Comparision of MHD Models for Aluminum Reduction Cells. Light Metals, 2006, 347-352.

4. G. V.Arkhipov and A. V.Rozin. The Aluminum Reduction Cell Closed System of 3D Mathematical Models. Light Metals 2005, 589-592.

5. M. V. Romerio and M. A. Secretan. Magneto-hydrodynamic equilibrium in aluminum electrolytic cells. Computer Physics Reports. 1986, 3: 327-360.June.

6. M. Dupuis, V. Bojarevics and D. Richard. Impact of the Vertical Potshell Deformation on the MHD Cell Stability Behavior of a 500 kA Aluminum Electrolysis Cell. Light Metals 2008, 409-412.

7. Feng Naixiang. New Cathodes in Aluminum Reduction Cells. Light Metals 2010, 405-408.

8. Dagoberto S. Severo, Andre F. Schneider, Elton C. V. Pinto, et al. Modeling Magnetohydrodynamics of Aluminum Electrolysis Cells with ANSYS and CFX. Light Metals 2005, 475-480.

9. ZHANG Hehui, ZHANG Hongliang, LI Jie, et al. The Use of Vortex Method in the Analysis of Multiphase Flow in Aluminum Reduction Cells. Light Metals 2012: 869-873.

10. N. X. Feng, Y. F. Tian, J. P. Peng, et al. New Cathodes in Aluminum Reduction Cells. Light Metals 2011, 191-197.

11. V. Potocnik, F. Laroche. Comparison of Measured and Calculated Metal Pad Velocities for Different Prebake Cell Design. Light Metals 2001, 419-425.

12. Zhang Xiaobo, Simulation of Electromagnetic Field and Interface Wave of Electrolyte/Aluminum in Aluminum Reduction Cell with Novel Cathode Structure. Shenyang, Northeastern University, 2011.

13. Zhou J., Adrian R. J., Balachandar S., Autogeneration of Near-wall Vortical Structures in Channel Flow. Physics of Fluids, 1996, 8(1): 288-290.